

Quantum control of a model qubit based on a multi-layered quantum dot

Alejandro Ferrón,^{1, a)} Pablo Serra,^{2, b)} and Omar Osenda^{2, c)}

¹⁾*Instituto de Modelado e Innovación Tecnológica (CONICET-UNNE),
Avenida Libertad 5400, W3404AAS Corrientes, Argentina*

²⁾*Facultad de Matemática, Astronomía y Física, Universidad Nacional de
Córdoba and IFEG-CONICET, Ciudad Universitaria, X5016LAE Córdoba,
Argentina*

(Dated: 1 August 2018)

In this work we present a model qubit whose basis states are eigenstates of a multi-layered quantum dot. We show that the proper design of the quantum dot results in qubit states that have excellent dynamical properties when a time-dependent driving is applied to it. In particular, it is shown that a simple sinusoidal driving is sufficient to obtain good quality Rabi oscillations between the qubit states. Moreover, the switching between states can be performed with very low leakage, even under off-resonance conditions. In this sense, the quantum control of the qubit is robust under some perturbations and achieved with simple means.

PACS numbers: 73.21.Ac,73.22.-f,73.22.Dj

^{a)}Electronic mail: aferron@conicet.gov.ar

^{b)}Electronic mail: serra@famaf.unc.edu.ar

^{c)}Electronic mail: osenda@famaf.unc.edu.ar

I. INTRODUCTION

Since Loss and DiVincenzo proposed the utilization of quantum dots as the physical implementation of the qubit¹, there has been a huge amount of work devoted to tackle the numerous and subtle difficulties involved in the problem. There are some excellent reviews^{2,3} and books⁴ that summarize the progress experimented by the field, but it is extremely difficult to keep up with the new developments.

As much as any other proposal to implement a qubit, the spin degree of freedom of an electron trapped in a quantum dot (QD), the original proposal made by Loss and DiVincenzo, must face a number of challenges owed to the intrinsic physics that governs its behavior as a qubit. Not to mention the challenges offered by other physical implementations that try to catch the attention of the community⁴. The double quantum dot scheme⁵ was devised to circumvent the unavoidable decoherence induced by the interaction between the angular momentum of the electron with the nuclear spins of the atoms that form the QD⁶. For this scheme, the realization of multiple qubit quantum gates has been shown⁷. Nevertheless, since the coupling between single QD's seems a bit problematic and maybe even more involved in the double QD scheme, there has been a number of proposal showing that it is possible to implement quantum control and refocusing techniques in single quantum dots to restore the role of the single QD as a bona fide qubit. This, together with techniques designed to distinguish between spatial states of the trapped electron, make interesting again the search of new one-electron structures that can be controlled with the exquisite precision required for the quantum information tasks.

The control of quantum systems, at least when the decoherence mechanisms are absent or “turned-off”, is implemented using pulses of external fields or manipulating an adequate parameter. A complete knowledge of the spectrum allows the use of “navigating methods” that make possible going from (almost) any initial state to the desired target state⁸. Nevertheless, the most used approach to achieve the switching between the two qubit basis states is the optimal control theory^{9,10}. The application of Krotov’s algorithm⁹ usually leads to speedups of the transition time. This method has successfully been applied to one-^{11,12} and two-electron quantum dots¹³, allowing fast charge transfer with larger fidelities than the obtained with simpler sinusoidal pulses. As much promising as the optimized pulse method seems, the introduction of a complex modulation of the control field necessarily introduces

a host of new error sources that have not been properly analyzed. In this sense, achieving a good control of the switching between states of a quantum dot without resorting to a complicated pulse sequence is worth of study, and is the aim of this work.

Recently, it has been shown that multi-layered quantum dots can be designed to selectively modulate the spatial extent of the electronic density of its eigenstates^{14,15}. This feature, together with the dipole selection rule permits, as we will show, the design of a quantum dot with two states that can be switched, robust and efficiently, using only sinusoidal pulses. These two states are the basis states of our model qubit. Using high-precision ab-initio numerical calculations and exact solutions, where available, we aim to study the spectrum, eigenstates of the quantum dot and dynamical properties of the qubit.

The paper is organized as follows, in Section II a realistic multi-layered quantum dot model is presented and qualitatively analyzed. In Section III the properties of the eigenvalues and eigenstates of the model are obtained. The study of the spatial extent of the eigenstates allows the identification of potential qubit basis states. The time evolution of the quantum state when the system is driven by an external sinusoidal radio frequency field (rf) is the subject of Section IV. It is shown that the sinusoidal driving is enough to obtain an excellent switching between the qubit basis states with very low probability leakage, making unnecessary the utilization of complicated envelope functions as is customary in optimal control theory. The stability of the qubit oscillations is also tested considering the effect of off-resonance driving. In Section V we briefly present a different model potential that also define an excellent qubit, whose properties are analyzed through the lines drawn in Sections II, III, and IV. Finally, we discuss our results in Section VI.

II. THE MODEL

In the Effective Mass Approximation, the Hamiltonian of trapped particles assumes a simple form since the many-body interactions are reduced to a bounding potential. In a spherical layered quantum dot, where each layer is made of a different material, the bounding potential is given by the conduction band off-sets of each material. Figure 1 shows, schematically, the radial profile of the bounding potential for a quantum dot made of two different materials. The basic structure consists of a central core and two wells separated by a barrier¹⁴.

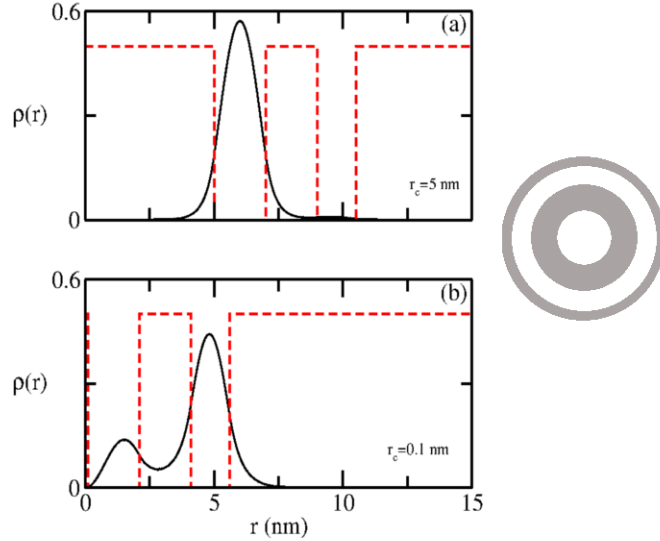


FIG. 1. (Color on-line) a) The electronic density for a quantum state well localized in the innermost potential well of a layered quantum dot. The radial step-like potential given by Equation 1 is also shown (red dashed line). b) The electronic density jumps from the innermost potential well to the outermost one when the radius of the quantum dot central core is changed. The target-like pattern to the right of the figure corresponds to the cross-section of the quantum dot, the grey zones correspond to both potential wells, while the central core, and the barrier are depicted with white.

Despite its simplicity, the piecewise potential takes into account a number of experimental features and allows the formulation of accurate and simple models for many nano-structures. The current semiconductor technology permit the fabrication of layered structures where the radius of each layer can be tuned with great precision. Figure 1 also shows the qualitative behavior of a given eigenstate, when the central core is wide enough the electronic density is mostly located in the inner potential well, conversely, when the radius of the central core is diminished the electronic density jumps to the outermost potential well for a certain critical value. So, changing the quantum dot architecture is equivalent to choose between different spectra and sets of eigenstates, whose physical properties can be dramatically changed just

altering the design of the quantum dot. In particular, the change in the spatial extent of low lying eigenstates and the modulation of the oscillator strength associated to these eigenstates was analyzed in the work by Ferrón *et al.*¹⁴.

More precisely, in this work the bounding potential considered is given by

$$V_c(r) = \begin{cases} V_0, & r < r_c; (ZnS), \\ 0, & r_c \leq r < r_1; (CdSe), \\ V_0, & r_1 \leq r < r_2; (ZnS), \\ 0, & r_2 \leq r < r_3; (CdSe), \\ V_0, & r \geq r_3; (ZnS). \end{cases} \quad (1)$$

where $V_0 = 0.9 \text{ eV}$ which corresponds to the band offset between CdSe and ZnS, while the effective masses are $m_{e,CdSe}^* = 0.13m_e$ and $m_{e,ZnS}^* = 0.28m_e$, m_e is the mass of the bare electron¹⁶.

Since we are interested in the properties of a one electron quantum dot when it is driven by an external field, the Hamiltonian takes the form

$$H = H_0 + V_{ext}(\vec{r}, t) \quad (2)$$

where

$$H_0 = -\frac{\hbar^2}{2} \nabla \left(\frac{1}{m(\mathbf{r})} \right) \nabla + V_c(r), \quad (3)$$

where $m(\mathbf{r})$ is the position-dependent effective mass of the electron, and the bounding potential is given in 1. The kinetic energy term in Equation 3 preserves the Hermitian character of the Hamiltonian operator when the mass is position dependent¹⁷. In the present case the mass a step-like function of the radial coordinate.

III. SPECTRUM AND EIGENSTATES

The spectrum and eigenstates of Hamiltonian 3 can be obtained exactly or numerically. In any case, the problem has spherical symmetry so the eigenvalues depend on two quantum numbers, (n_r, ℓ) , where n_r is radial quantum number, or the number of nodes of the radial eigenfunction, and ℓ is the orbital angular momentum quantum number. On the other hand,

note that since the exact solution of the eigenvalue problem involves the roots of transcendental equations, it can be difficult to figure out how many quasi-degenerate eigenvalues has the problem. This difficulty is particularly cumbersome for large values of r_c . Conversely, the variational methods detect fairly well almost degenerate eigenvalues, so the data shown in this Section was double-checked comparing the results from the numerical and analytical procedures,

The numerical solutions were obtained using B-splines basis sets, which are well suited to implement the boundary conditions imposed by the step-like nature of the potential and the effective mass. Besides, B-splines results are very accurate in comparison with calculations based on Gaussian, Hylleraas and finite-element basis sets¹⁸.

To use the B-splines basis, the normalized one-electron orbitals are given by

$$\phi_n(r) = C_n \frac{B_{n+1}^{(k)}(r)}{r}; \quad n = 1, \dots \quad (4)$$

where $B_{n+1}^{(k)}(r)$ is a B-splines polynomial of order k . The numerical results are obtained by defining a cutoff radius R , and then the interval $[0, R]$ is divided into I equal subintervals. B-spline polynomials¹⁹ (for a review of applications of B-splines polynomials in atomic and molecular physics, see ref.²⁰) are piecewise polynomials defined by a sequence of knots $t_1 = 0 \leq t_2 \leq \dots \leq t_{2k+I-1} = R$ and the recurrence relations

$$B_i^{(1)}(r) = \begin{cases} 1 & \text{if } t_i \leq r < t_{i+1} \\ 0 & \text{otherwise,} \end{cases} \quad (5)$$

$$B_i^{(k)}(r) = \frac{r - t_i}{t_{i+k-1} - t_i} B_i^{(k-1)}(r) + \frac{t_{i+k} - r}{t_{i+k} - t_{i+1}} B_i^{(k-1)}(r) \quad (k > 1). \quad (6)$$

In this work, we use the standard choice for the knots in atomic physics²⁰ $t_1 = \dots = t_k = 0$ and $t_{k+I} = \dots = t_{2k+I-1} = R$. We choose an equidistant distribution of inside knots. The constant C_n in Eq.(3) is a normalization constant obtained from the condition $\langle n|n \rangle = 1$,

$$C_n = \frac{1}{\left[\int_0^{R_0} \left(B_{n+1}^{(k)}(r) \right)^2 dr \right]^{1/2}}. \quad (7)$$

Because $B_1(0) \neq 0$ and $B_{I+k-1}(R) \neq 0$, we have $N = I + k - 3$ orbitals corresponding to B_2, \dots, B_{I+k-2} . In all the calculations we used the value $k = 5$, and, we do not write the index k in the eigenvalues and coefficients.

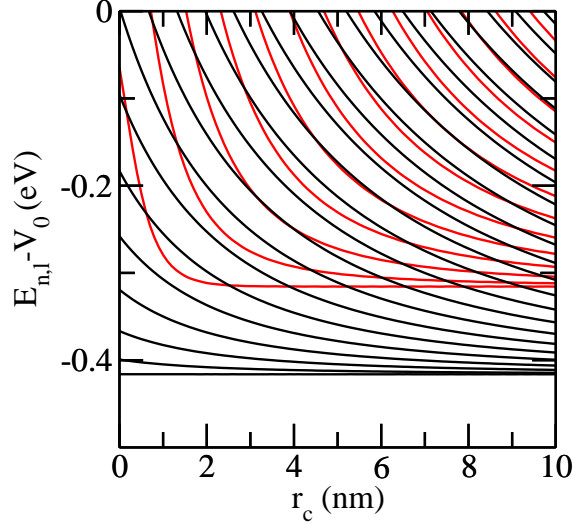


FIG. 2. (Color on-line) The spectrum of a typical layered quantum dot as a function of the inner core radius, r_c . The radius of each layer is, $r_1 = r_c + 0.8$, $r_2 = r_1 + 3.5$, and $r_3 = r_2 + 1$, all in nanometers. The black solid lines correspond (from bottom to top) to eigenvalues with quantum numbers $(n_r = 0, \ell)$, $\ell = 0, 1, 2, \dots, 22$, while the red solid lines correspond to (from bottom to top) eigenvalues with quantum numbers $(n_r = 1, \ell)$, $\ell = 0, 1, 2, \dots, 12$.

Figure 2 shows the spectrum of a double-well quantum dot as a function of the central core radius, the width of the two wells and the barrier are kept constant, so $r_1 = r_c + 0.8\text{nm}$, $r_2 = r_1 + 3.5\text{nm}$ and $r_3 = r_2 + 1\text{nm}$. As can be appreciated, the spectrum is quite complicated and there is not a couple of energy values well separated from the others, which is a common criterion to identify possible basis eigenstates for a qubit. As we will show, the availability of a couple of eigenstates that can be easily switched with a simple pulse depends not only on the characteristics of the spectrum, but also in the eigenstates spatial extent.

Figure 3 shows the electronic density corresponding to all the bounded eigenstates of two similar devices. Panel a) corresponds to a device with only two eigenstates well localized in the innermost potential well, while panel b) shows a device with three eigenstates localized in the innermost potential well. The two devices only differ in the central core radius size, it is bigger for the b) case. The radii of both devices are, Device 1: $r_c = 1$ nm, $r_1 = 1.8$ nm, $r_2 = 5.3$ nm and $r_3 = 6.3$ nm. Device 2: $r_c = 2$ nm, $r_1 = 2.8$ nm, $r_2 = 6.3$ nm and $r_3 = 7.3$ nm.

In both cases the eigenstates localized in the inner potential well have different angular

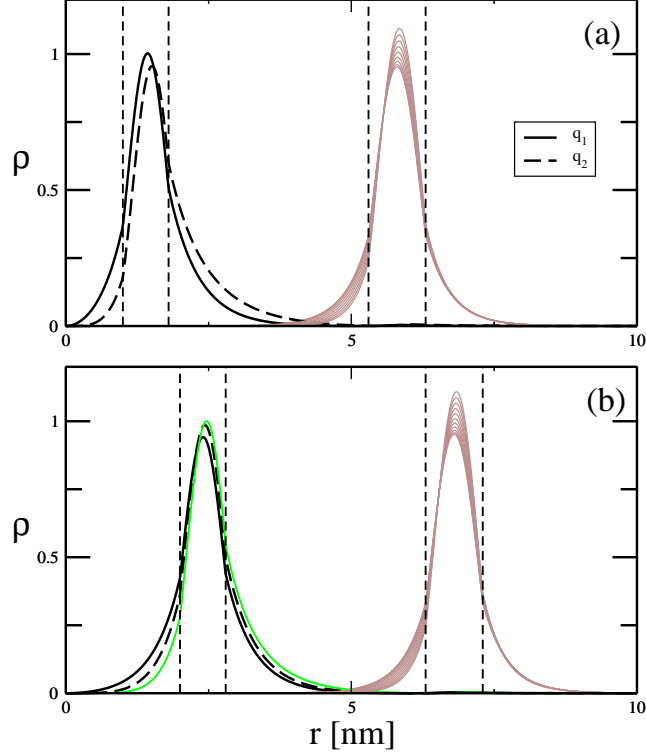


FIG. 3. (Color on-line) Electronic densities for the ground and excited states for two different CdSe/ZnS devices. (a) Device 1, (b) Device 2. The electronic densities of the eigenstates corresponding to the qubit states are denoted with q_1 and q_2 , which have quantum numbers $(1, 0)$ and $(1, 1)$, respectively. The black dashed vertical lines show the positions of the barriers and wells of the quantum dot. Both Devices are particular cases of the layered quantum dot whose spectra are depicted in Figure 2.

momentum quantum numbers, in a) $\Delta\ell = 1$. Actually, in the Device 1 case, the qubit lower state has quantum numbers $n_r = 1$ and $\ell = 0$, while the higher one has $n_r = 1$ and $\ell = 1$, while in the Device 2 case the third state has $n_r = 1$ and $\ell = 2$. Figure 3 shows two remarkable facts, i) the number of eigenstates localized in a given potential well can be chosen for realistic quantum dots parameters and, ii) the number of states of election is pretty stable against small changes in the device's parameters (see also Figure 2). However, as we will show latter a change in the number of states localized in the potential well of interest can produce a huge change in the dynamical behavior once a external driving is applied to the device.

On the other hand, despite that we mostly present results for particular sets of param-

eters (effective masses, radii, etc.) the physical traits that, at some extent, guarantee the existence of a small number of eigenstates well localized in a multi-well potential are fairly general. Indeed, later on we will show an example with a continuous bounding potential whose spectrum, eigenstates and dynamical behavior are strikingly similar to those of the devices with step-like potentials.

IV. SINUSOIDAL DRIVING OF THE ELECTRON

The most simple non-trivial driving, both from an numerical and experimental point of view, that can be applied to the trapped electron is

$$V_{ext}(\vec{r}, t) = A_0 \cos(\omega t)z \quad (8)$$

where A_0 and ω are the strength and the frequency of the driving, respectively. The time-dependent potential, Equation 8, models the effect of a time-periodic spatially constant electric field applied in the z direction. As the potential Equation 8 depends on z , the dipole selection rules impose transitions between eigenstates that differ in orbital angular momentum, $\Delta\ell = \pm 1$.

The time evolution of the electron quantum state is governed by the Schrödinger equation,

$$i\hbar \frac{\partial \Psi}{\partial t} = H\Psi \quad (9)$$

where Ψ is the quantum state and H is the Hamiltonian in Equation 2. Since we want to analyze the behavior of the devices presented in the previous Sections as qubits, we will study the electron quantum state evolution, taking as initial condition the lowest eigenstate that is localized in the innermost potential well, from now on the $|0\rangle$ state of our putative qubit, this state has $\ell = 0$. The other qubit basis state, $|1\rangle$ is the eigenstate with $\ell = 1$ that is also localized in the innermost potential well. Ideally, to qualify as a qubit, a physical system would perfectly switch between the two basis states under the appropriate driving, *i.e.* if $|c_{q1}|^2$ and $|c_{q2}|^2$ are the time dependent probabilities that the electron is in the $|0\rangle$ or in the $|1\rangle$ state, respectively, then $|c_{q1}|^2 + |c_{q2}|^2 = 1$.

Except for ideal two level systems, there is a finite probability that after a switching operation $|c_{q1}|^2 + |c_{q2}|^2 < 1$, *i.e.* the qubit leaks probability. The *leakage*, defined as $1 - (|c_{q1}|^2 + |c_{q2}|^2)$, is a good measure to judge the performance of a given system as a qubit²¹. In

actual physical systems, the leakage has a twofold origin, the driving used to switch between the basis states produces transitions to other levels besides the ones of interest, and the interaction with the environment. In this work we will only analyze the former without considering the possibility of ionization, so the electron remains bounded while the driving is applied.

The material that follows is quite standard, nevertheless we include it for the sake of completeness. Writing the quantum state as a superposition of all the eigenstates

$$\Psi(\vec{r}, t) = \sum c_n(t) e^{-iE_n t/\hbar} \Phi_n(r) \quad (10)$$

where

$$H_0 \Phi_n(r) = E_n \Phi_n(r), \quad (11)$$

is the eigenvalue problem, and replacing Equation 10 in the Schrödinger equation, 9, we get

$$\sum c_n(t) e^{-iE_n t/\hbar} H \Phi_n = i \sum \frac{\partial}{\partial t} (c_n(t) e^{-iE_n t/\hbar}) \Phi_n. \quad (12)$$

which can be solved for $c_k(t)$ using the orthogonality of the Φ_n 's²²,

$$i \frac{\partial c_k(t)}{\partial t} = \sum_{n=0}^{\infty} c_n(t) \langle \Phi_k | V_{ext} | \Phi_n \rangle e^{i\omega_{kn} t}. \quad (13)$$

Introducing the explicit for of the external driving, Equation 8, we get that

$$i \frac{\partial c_k(t)}{\partial t} = A_0 \cos(\omega t) \sum_{n=0}^{\infty} c_n(t) Z_{kn} e^{i\omega_{kn} t} \quad (14)$$

where $\omega_{kn} = (E_k - E_n)/\hbar$, and

$$Z_{kn} = \langle \Phi_k | z | \Phi_n \rangle, \quad (15)$$

clearly, the time-dependent probability that a given state, say k , is occupied at time t is given by $|c_k(t)|^2$

Equation 14 shows that, even if the driving is in resonance with the frequency $\omega_{res} = (E_{q2} - E_{q1})/\hbar$, there are transitions to all the bounded states allowed by the dipole selection rules so, unless somehow the matrix elements Z_{kn} preclude this possibility, for large enough time all the terms in the superposition Equation 10 will have non-negligible contributions. This fact, inevitably, produces a large and undesirable leakage.

The points made above suggest that a proper design of the nano-structure would lead to negligible matrix elements Z_{kn} for the unwanted transitions. This is the reason to choose

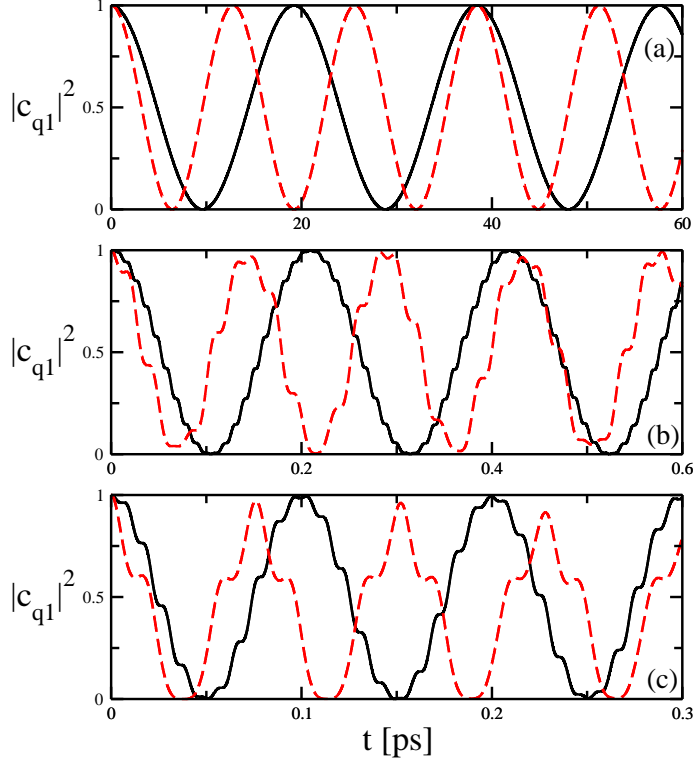


FIG. 4. (Color on-line) Time dependent probability of finding the system in the lower state of the qubit ($|c_{q1}|^2$) for different devices and for an rf field pulse of strength A_0 at the resonant frequency $\omega_{res} = (E_{q2} - E_{q1})/\hbar$. The system is prepared in the lower qubit state for $t = 0$. The black solid line corresponds to the time dependent probability for the Device 1 and red dashed line corresponds to the time dependent probability for the Device 2. (a) $A_0 = 0.27$ meV/nm, (b) $A_0 = 25.0$ meV/nm and (c) $A_0 = 52.5$ meV/nm.

structures that single out a couple of eigenstates whose spatial extent is quite different from all the other ones since, clearly, this is a economical way to reduce the transitions to eigenstates that are not those of the qubit. The naive picture that says that the basis states of a qubit can be chosen as two well separated states of a physical system is really hard to be found, in particular when the requirements of fast enough operations also must be accomplished¹⁴. From a physical point of view, to obtain faster operation times it is necessary to draw on stronger external drivings. By two well separated states, it is meant that the energy difference between any other state with the qubit states is much larger than the energy difference between the qubit states.

The matrix elements Z_{kn} can be obtained for all the bounded states of Devices 1 and

2 with very high precision so, the time evolution of the electronic quantum state results from the integration of Equation 14. The numerical integration was performed using high precision Runge-Kutta algorithms, taking into account all the bounded states that each device possess.

Figure 4 shows the time evolution of the occupation probability of one of the qubit basis states, the initial condition is $\Psi(t = 0) = |q\rangle$. The Figure shows the time evolution for three different driving strengths and two Devices, those whose eigenstates electronic densities are shown in Figure 3. Clearly, as the driving increases its value, the time evolution of the state becomes less and less harmonic. Anyway, for all the driving strengths shown, a fast switching between states can be easily achieved. The departure from a simple oscillatory behavior observed for larger driving strengths, and that $|c_q(t)|^2 < 1$ for $t > 0$, shows that the driving is producing a superposition of many different eigenstates. On the other hand, from the three panels of Figure 4, the dependence of the switching time on the driving strength is manifest.

As has been said above, that $|c_q(t)|^2$ does not reach the unity for $t > 0$, is manifestation of the probability leakage, *i.e.* the state does not switch perfectly between the two qubit basis states. Anyway, for systems with a finite number of states, there is a finite probability that the state of the system returns to the initial state for a large enough evolution time. A potential well has indeed a finite number of eigenstates and, in many cases, the numerical integration of Equations 14 imposes a further reduction of the number of eigenstates effectively considered. For these reasons it is useful to introduce time-averaged quantities to qualify the dynamical behavior of the system.

Together with the instantaneous leakage, $1 - (|c_{q1}|^2 + |c_{q2}|^2)$, it is customary to introduce the time-averaged Leakage, L_p , which is defined as

$$L_p = \frac{1}{T} \int_t^{t+T} (1 - (|c_{q1}(t')|^2 + |c_{q2}(t')|^2)) dt', \quad (16)$$

where T is a large enough time that, in principle, can be taken equal to several periods of the external driving. Figure 5 shows the behavior of the time-averaged Leakage for the two Devices previously defined as a function of the strength of the external driving. As can be appreciated, the time-averaged Leakage depends quadratically on the driving strength. On the other hand, Figure 5 shows that, despite that Device 2 differs from Device 1 in just one single eigenstate localized in the innermost potential well, the Leakage of both devices differ

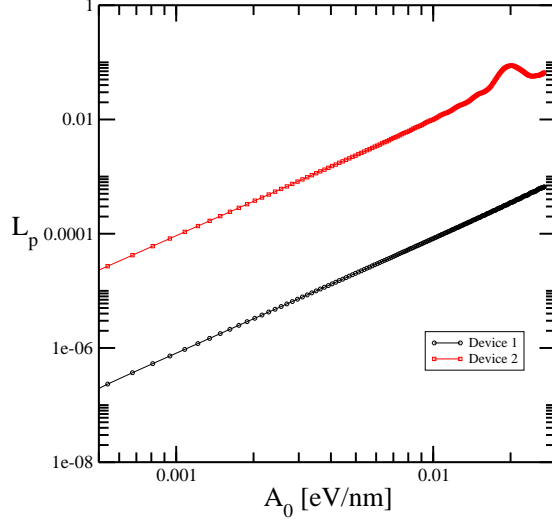


FIG. 5. (Color on-line) Time-averaged leakage L_p for an rf field pulse of strength A_0 at the resonant frequency $\omega_{res} = (E_{q2} - E_{q1})/\hbar$ as a function of the pulse strength for the Device 1 (black circle dots and line) and the Device 2 (red squared dots and line).

in two orders of magnitude. It is worth to remark here that the spectrum of both devices are, essentially, the same (see Figure 2).

The good performance of Device 1 as a qubit can be further emphasized, looking at the dynamical behavior of the quantum state, when the system is forced with an off-resonance driving.

Figure 6 shows the behavior of the Leakage as a function of the frequency of the external driving. It is assumed that the driving potential has the same properties that the one in Equation 8. The Figure shows the data obtained for the two larger driving strengths showed in Figure 4 since these two are the worse cases. As can be appreciated, for the smaller driving strength the driving frequency can be off-resonance up to $\pm 10\%$ without changing appreciably the Leakage. The size of this tolerance interval is closely related to the ratio between the eigen-energies differences with the driving strength. For the larger driving, the tolerance interval for frequencies smaller than ω_{res} is, at least, as larger as the tolerance interval for the smaller driving. The peaks in both sets of data signal that the transition probability to other states, which are not those of the qubit, gets bigger, spoiling the switching between the qubit states.

It is worth to mention here that when the architecture of the quantum dot separates

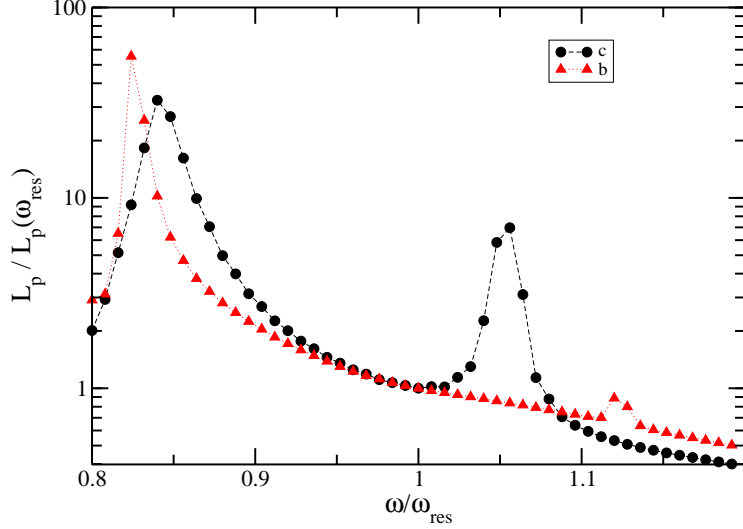


FIG. 6. (Color on-line) The Leakage experimented by the Device 1 when the external driving is off-resonance. Note that both axis scale are normalized to the on-resonance values. The (red) triangle dots correspond to the a driving strength of $A_0 = 25.0$ meV/nm and the (black) solid dots to $A_0 = 52.5$ meV/nm, respectively. These driving strengths correspond to the cases b) and c) of Figure 4

two eigenstates, the residual leakage is produced by the small overlap between the qubit states and all the other eigenstates. Actually, because the small barrier that separates the potential wells, there is a non-negligible portion of the qubit states that lies in the outermost well. A better design would reduce or eliminate this portion enhancing the good behavior of the qubit. In the next Section we present a different model potential that possess exactly all the desirable properties that we have mentioned so far: separates in a potential well the two lowest lying eigenstates, and reduces the overlap between the qubit states and the other states to almost negligible values. Regrettably the model potential, and the parameters that characterize it, does not correspond to a nano-device already proposed. Anyway, since we have tested only a very limited set of options, it is possible that the discussion of the ideas presented here helps to find better designs for qubits based on multi-layered quantum dots.

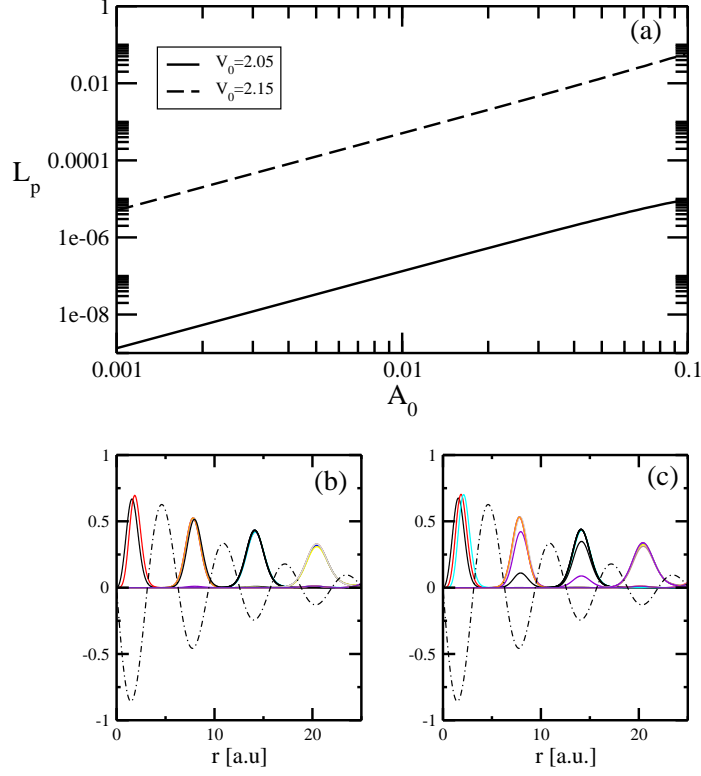


FIG. 7. (Color on-line) a) The Leakage *vs* the driving strength A_0 , the value of V_0 is shown in the figure, while $\omega = 1$ and $\gamma = 0.1$. The black solid line corresponds to the device shown in panel b) and the dashed black line to the device shown in panel c). Note that the devices differ in the number of eigenstates localized in the innermost well, two and three states in panels b) and c), respectively. In panels b) and c) the black dashed line represents the decaying sinusoidal potential, in units of A . The color lines correspond to the electronic densities of several eigenstates.

V. OTHER SYSTEMS

So far, we have not been able to find an adequate set of parameters (radii, materials and so on) to design a quantum dot model that separates as qubit states eigenstates with $n_r = 0$. The state with $n_r = \ell = 0$ has too many advantages to rule out too fast the search of a quantum dot such that one of the two separated eigenstates be it. By separated states we mean that two eigenstates are well localized in a given potential well, while all the other bounded eigenstates are localized in other potential wells.

Anyway, the separation of the lowest lying eigenvalue, $n_r = \ell = 0$, and an excited state

with $\ell = 1$ can be achieved in the potential

$$V_c(r) = -V_0 e^{-\gamma r} \sin(\omega r), \quad (17)$$

where V_0 , γ and ω are constants. The potential in Equation 17 has some common properties with step-like potentials like the one in Equation 1¹⁴. The parameters of the potential and its shape are quite different from those commonly found in nano-devices, so in this Section we use atomic units.

Figure 7 shows the Leakage suffered by the two “devices” depicted in panels b) and c) that has two and three states localized in the innermost well, respectively. The parameter that drives the change from two to three separated states is, in this case, V_0 . The two lowest lying eigenvalues have quantum numbers $(n_r = 0, \ell = 0)$ and $(n_r = 0, \ell = 1)$. We call V_0^c the critical value such that for $V_0 < V_0^c$ there are only two well localized states in the innermost well. For $V_0 > V_0^c$ there are more than two localized states in the innermost well, in our case $V_0^c \approx 2.09$

The eigenvalues and eigenstates of the one-electron Hamiltonian with potential 17 were obtained approximately using the FEM-DVR method (finite-element method plus discrete variable representation), see²³⁻²⁵.

As can be seen in Figure 7 a) the Leakage of the device with three separated states is larger than the leakage suffered by the device with only two states separated. Again, the Leakage is a quadratic function of the driving strength, A_0 .

The influence of the number of separated states in the Leakage can be put further in evidence analyzing its behavior when V_0 is swept from a smaller value than the critical to a larger value than V_0^c . This behavior is shown in Figure 8. As can be appreciated from panel a) there is a sudden change in the Leakage around the critical value, in fact the Leakage changes three orders of magnitude when V_0 goes from smaller values than the critical to larger ones, irrespective of the driving strength, at least for the range of values analyzed. The jump can be rightly attributed to the presence of other states than those of the qubit since the others quantities involved (in the Leakage) are continuous, for example, Figure 8 b) shows the behavior of the resonance frequency as a function of V_0 .

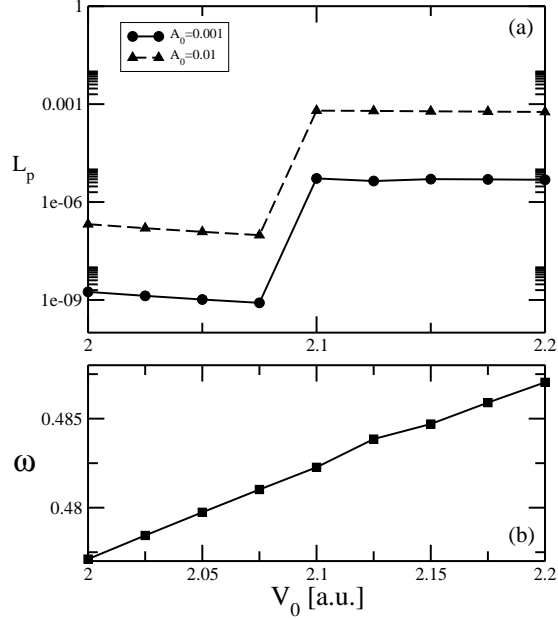


FIG. 8. (a) Time-averaged leakage L_p for an rf field pulse of strength $A_0 = 0.001$ (black solid dots and line) and $A_0 = 0.01$ (triangle dots and dashed line), at the resonance frequency, as a function of V_0 . (b) The resonance frequency as a function of V_0 .

VI. DISCUSSION AND CONCLUSIONS

The ability of multi-wells and barriers spherical potentials to separate a subset of eigenstates in a potential well could be a tool to better designed nano-devices. This capacity has not been yet systematized, there are not exact results or theorems that allow a systematic search of model potentials with all the desirable characteristics, despite it seems fairly general.

As has been said above, once two eigenstates are separated in a potential well from all the other eigenstates, the residual leakage observed during the switching between them is attributable to the overlap between the qubit states and the other eigenstates. A higher barrier between the potential wells could reduce the overlap but, so far, we do not know of quantum dots built from three different semiconductor compounds.

The advantage of the ground state as one of the qubit basis state is obvious, it can be pinpointed by cooling methods while other states require more sophisticated means to force the electron to actually occupy one of them.

Our results contribute to show that there are, yet, a lot of improvements that can be

made to the design of qubits based on semiconductor quantum dots. The huge amount of materials and geometries offer ample possibilities to tackle the drawbacks that have marred the development of a reliable quantum dot based qubit. Of course the decoherence induced by the spin-orbit interaction, not considered in this work, stills remains as the heavier challenge. To minimize the effects of spin-orbit interaction the qubit states should be located in a potential well made of the material with the lowest spin-orbit interaction strength possible.

ACKNOWLEDGEMENTS

We would like to acknowledge SECYT-UNC, CONICET and MinCyT Córdoba for partial financial support of this project. A.F. likes to acknowledge PICT-2011-0472 for partial financial support of this project. O.O. likes to acknowledge the hospitality at the Instituto de Modelado e Innovación Tecnológica (CONICET-UNNE), where this project started.

REFERENCES

- ¹D. Loss and D. P. DiVincenzo, Phys. Rev. A **57**, 120 (1998)
- ²Stephanie M. Reimann and Matti Manninen, Rev. Mod. Phys. **74**, 1283 (2002)
- ³L. P. Kouwenhoven, D. G. Austing, and S. Tarucha, Rep. Prog. Phys. **64**, 701 (2001)
- ⁴S. L. Braunstein, H-K Lo, and P. Kok (Eds.), *Scalable Quantum Computers* (Wiley-VCH Verlag, Berlin, 2001)
- ⁵D.P. DiVincenzo, Science **309**, 2173 (2005)
- ⁶R. Petta, A. C. Johnson, J. M. Taylor, E. A. Laird, A. Yacoby, M. D. Lukin, C. M. Marcus, M. P. Hanson, A. C. Gossard, Science **309**, 2180 (2005).
- ⁷R. Brunner, Y.-S. Shin, T. Obata, M. Pioro-Ladrière, T. Kubo, K. Yoshida, T. Taniyama, Y. Tokura, and S. Tarucha, Phys. Rev. Lett. **107**, 146801 (2011).
- ⁸G. Murgida, D. A. Wisniacki and P. Tamborenea, Phys. Rev. Lett **99**, 036806 (2007)
- ⁹V. F. Krotov, *Global Methods in Optimal Control Theory*, Monographs and Textbooks in Pure and Applied Mathematics Vol. **195** (Marcel Dekker, New York, 1996).
- ¹⁰S. E. Sklarz and D. J. Tannor, Phys. Rev. A **66**, 053619 (2002).

- ¹¹E. Räsänen, A. Castro, J. Werschnik, A. Rubio, and E. K. U. Gross, Phys. Rev. Lett. **98**, 157404 (2007)
- ¹²E. Räsänen, A. Castro, J. Werschnik, A. Rubio, and E. K. U. Gross, Phys. Rev. B **77**, 085324 (2008)
- ¹³L. Sælen, R. Nepstad, I. Degani, and J. P. Hansen, Phys. Rev. Lett. **100**, 046805 (2008)
- ¹⁴A. Ferrón, P. Serra and O. Osenda, Phys. Rev. B **85**, 165322 (2012)
- ¹⁵H. Taş and M. Şahin, J. Appl. Phys. **111**, 083702 (2012)
- ¹⁶Xi Zhang, Guiguang Xiong, Xiaobo Feng, Physica E **33**, 120 (2006)
- ¹⁷F. Stern and S. Das Sarma, Phys. Rev. B **30**, 840 (1984)
- ¹⁸P. Serra and S. Kais, J. Phys. B **45**, 235003 (2012).
- ¹⁹C. de Boor, *A Practical Guide to Splines* (Springer, New York, 2001)
- ²⁰H. Bachau, E. Cormier, P. Decleva, J. E. Hansen, and F. Martin, Rep. Prog. Phys. **64**, 1815 (2001).
- ²¹A. Ferrón and D. Domínguez, Phys. Rev. B **81**, 104505 (2010).
- ²²E. Merzbacher, *Quantum Mechanics* (2nd Edition, Wiley, New York, 1970)
- ²³C. Y. Lin and Y. K. Ho, J. Phys. B: At. Mol. Opt. Phys. **45**, 145001 (2012)
- ²⁴Liang Tao, C. W. McCurdy, and T. N. Rescigno, Phys. Rev. A **79**, 012719 (2009)
- ²⁵T. N. Rescigno and C. W. McCurdy, Phys. Rev. A **62**, 032706 (2000)